

# Quantum Hall and Light Responses in a 2D Topological Semimetal

Karyn Le Hur and Sariah Al Saati<sup>1</sup>

<sup>1</sup>*CPHT, CNRS, Institut Polytechnique de Paris, Route de Saclay, 91120 Palaiseau, France*

We have recently identified a protected topological semimetal in graphene which presents a zero-energy edge mode robust to disorder and interactions. Here, we address the characteristics of this semimetal and show that the  $\mathbb{Z}$  topological invariant of the Hall conductivity associated to the lowest energy band can be equivalently measured from the resonant response to circularly polarized light resolved at the Dirac points. The (non-quantized) conductivity responses of the intermediate energy bands, including the Fermi surface, also give rise to a  $\mathbb{Z}_2$  invariant. We emphasize on the bulk-edge correspondence as a half-topological protected semimetal, i.e. one spin-population polarized in the plane is in the insulating phase related to the robust edge mode while the other is in the metallic regime. The quantized transport at the edges is also equivalent to a  $\frac{1}{2} - \frac{1}{2}$  conductance for spin polarizations along  $z$  direction. We also build a parallel between the topological Hall response through the quantized light response at the Dirac points and a pair of half numbers (half Skyrmions).

## I. INTRODUCTION

At the heart of topological aspects in condensed-matter systems is the nontrivial nature of the wavefunction in reciprocal space associated to the band structure of a crystal. Indeed, one of the key theoretical tools underlying the study of topological matter is the notion of topological invariants which have direct consequences on the dynamics of the material. The main topological invariant of interest is the Chern number associated to the Brillouin Zone of the material. Remarkably, this integer Chern number was found to be directly related to the Hall conductivity of the material, showing a unique quantized behavior in units of the fundamental constant  $e^2/h$  [1, 2], accessible in quantum transport experiments. This topological number was also found to be equivalently accessible from the response of the material to circularly polarized light [3–5]. This topological response to circularly polarized light can also be equivalently resolved locally within the Brillouin zone [6]. The topological characterization can also be revealed from a local microscope i.e. a long transmission line transporting classical light [7].

Quantum spin Hall insulators are two-dimensional topological insulators which have gained prominence in the last two decades [8, 9]. Quantum spin Hall insulators are characterized by the presence of the spin Hall effect, where an electric current induces a transverse spin current due to intrinsic spin-orbit coupling. These spin Hall systems are most often theoretically described by two spin-polarized subsystems, called spin channels, which are related through time-reversal symmetry. A specific example is the case of the Kane-Mele model [10–14] in which the spin of the electron is a well defined quantum number labelling distinct energy bands. In this model, each spin channel hosts oppositely directed edge modes, referring then to the quantum spin Hall effect. This description in terms of counter-propagating spin channels is also valid for the Bernevig-Hughes-Zhang model [15]. The system then hosts a zero total Chern number and is equivalently described through a  $\mathbb{Z}_2$  topological spin Chern number related to the structure of the quantum

spin Hall current at the edges [10, 16]. Circularly polarized light can measure this topological  $\mathbb{Z}_2$  invariant related to the quantum spin Hall effect [6] and the parity symmetry [17] with a perfect quantization at the Dirac points on the honeycomb lattice associated to the zeros of the Pfaffian [11].

The classification of topological properties in terms of two distinct Pauli matrices, e.g. related to the two sublattices on the honeycomb lattice and to the two spin polarizations of an electron in the Kane-Mele model, was at the heart of our recent publication [18], in which we describe a possible generalization of nontrivial topological properties and robustness towards a specific class of two-dimensional (2D) topological semimetals realizable in graphene. The topological protection of this semimetal was shown through a robust zero-energy edge mode polarized along  $x$  direction in the energy spectrum. This was shown numerically in the presence of disorder and through a stochastic variational approach in the presence of interactions [5, 19, 20].

In this article, we study the bulk topological characteristics of this 2D semimetal in graphene and we present a precise correspondence with the quantum Hall conductivity and the response to circularly polarized light. In Sec. II, we recall the Hamiltonian and band structure of this system [18]. Applying the Kubo formula for the topological semimetal, in Sec. III, we check that the topological invariant of the lowest-energy band spin-polarized along  $x$  direction remains quantized for all the range of parameters in the sense of the quantum Hall response, revealing the existence of the edge mode. An interesting result found in Sec. IV is that the response to circularly polarized light resolved in frequency, corresponding to a resonance with the Dirac points, can equally reveal this quantized  $\mathbb{Z}$  topological marker associated to the lowest-energy band. In Sec. III we also derive the quantum Hall conductivity of the second-energy energy band and of the nodal ring region. We verify that these contributions are well defined, but these integrals of Berry flux of particles are not quantized reflecting the Fermi surface properties in agreement with the article by Haldane in 2004 [21]. Yet, we find that we can introduce a quan-

tized  $\mathbb{Z}_2$  topological marker to characterize the topological properties associated to the second-energy band and the Fermi surface. The light response at the Dirac points for the semimetal is equivalent to a pair of  $\frac{1}{2}$  topological numbers (half Skyrmions), linking then with the physics of the topological semimetal in the bilayer model related to the model of two entangled spheres [22, 23]. This semimetal was understood to host two channels of the Haldane model [24] as in the Kane-Mele model, revealing a  $\mathbb{Z}_2$  symmetry and halved transport at the edges. In the present study in one layer graphene, the bulk-edge correspondence in Sec. V will lead to the formation of a half topological semimetal when varying the chemical potential i.e. with one spin polarization showing a quantized conductance and one spin polarization showing a metallic behavior. The quantized transport at the edges along  $x$  direction is also equivalent to a  $\frac{1}{2} - \frac{1}{2}$  probability for each spin polarization along  $z$  direction showing a correspondence with the topological bilayer system [22, 23].

## II. PROTECTED TOPOLOGICAL SEMIMETAL

The model of the semimetal in one layer graphene [18] is related to the presence of an Haldane model associated to the two spin polarizations of an electron in the plane. We include a magnetic field, such that its direction is fixed parallel to the layer to induce Zeeman effects. The energy bands of the system will be then classified according to the two spin polarizations of an electron along  $x$  direction. In recent years, there have been many developments of proximity-induced topological phases of matter [25–28] and in particular on graphene/Transition-metal dichalcogenide (TMD) heterostructures [29, 30] with easily tunable parameters. Therefore, we can anticipate that there will be various equivalent ways to realize this topological semimetal in two dimensions through two sets of Pauli matrices related to the physics of heterostructures. The Hamiltonian of the two-dimensional (2D) topological semimetal can be written in tight-binding formalism in reciprocal space as [18]

$$\mathcal{H} = \sum_{\mathbf{k} \in BZ} \psi^\dagger(\mathbf{k}) \mathcal{H}(\mathbf{k}) \psi(\mathbf{k}) \quad (1)$$

with

$$\psi(\mathbf{k}) = (c_{A\mathbf{k}\uparrow}, c_{B\mathbf{k}\uparrow}, c_{A\mathbf{k}\downarrow}, c_{B\mathbf{k}\downarrow}) \quad (2)$$

$$\mathcal{H}(\mathbf{k}) = \mathbf{d}_{\mathbf{k}} \cdot \boldsymbol{\sigma} \otimes \mathbb{I} + r\mathbb{I} \otimes s_x, \quad (3)$$

where  $A$  and  $B$  label the two nonequivalent sites of the honeycomb lattice.

The Hamiltonian is written in terms of two sets of Pauli matrices:  $\boldsymbol{\sigma}$  acting on the Hilbert space  $\{|A\rangle; |B\rangle\}$  associated to the two sublattices  $A$ - $B$  and  $\mathbf{s}$  acting on  $\{|\uparrow_z\rangle; |\downarrow_z\rangle\}$  linked to the two spin polarizations of an electron in the direction perpendicular to the graphene layer.

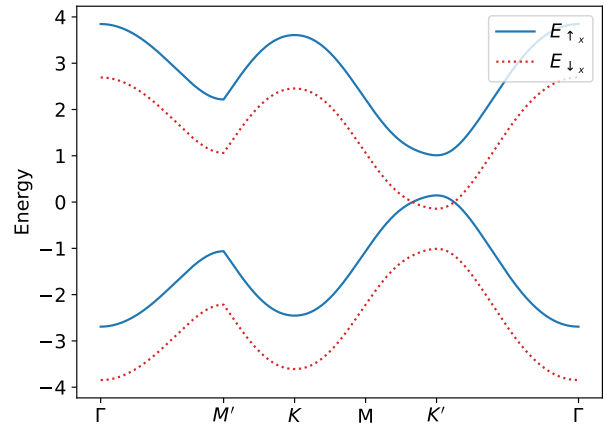


Figure 1. Color Online: Two-dimensional band structure of the system for a chosen path in the Brillouin zone with the spin polarizations associated to the energy bands shown in distinct colors. The parameters chosen for all panels are  $M = 3\sqrt{3}t/4$ ,  $r = t/\sqrt{3}$ ,  $t_2 = t/3$  with lattice spacing  $a = 1$ .

In this way, Zeeman effects occur through the  $x$  spin-Pauli matrix. We recall here that the  $d_x(\mathbf{k})$  and  $d_y(\mathbf{k})$  terms in the Bloch hamiltonian describe the kinetic terms of graphene whereas the  $d_z(\mathbf{k})$  term represents the topological term introduced first by Haldane in 1988 [24] giving rise to a mass inversion effect between the two Dirac points  $K$  and  $K'$  in the Brillouin zone, referring to the inversion of eigenstates related to the lower and upper energy bands when inverting the two Dirac points. From standard definitions, on the honeycomb lattice, we identify the respective components of the  $\mathbf{d}_{\mathbf{k}} = \mathbf{d}(\mathbf{k})$  vector

$$d_x(\mathbf{k}) = -t \sum_{i=1}^3 \cos(\mathbf{k} \cdot \boldsymbol{\delta}_i) \quad (4)$$

$$d_y(\mathbf{k}) = -t \sum_{i=1}^3 \sin(\mathbf{k} \cdot \boldsymbol{\delta}_i) \quad (5)$$

$$d_z(\mathbf{k}) = M + 2t_2 \sum_j \sin(\mathbf{k} \cdot \mathbf{b}_j), \quad (6)$$

where  $t > 0$  represents the hopping amplitude between nearest-neighbours  $A$  and  $B$ , and  $\boldsymbol{\delta}_i$  represents the three nearest-neighbour vectors linking these sites. For simplicity, we assume here that the second nearest-neighbor hopping term is purely imaginary and equal to  $it_2$  (with  $t_2 > 0$ ) in the Haldane model. This term is the one giving rise to topological properties in graphene, and can be implemented using circularly polarized light [18, 31] as achieved in recent years [32]. Then,  $\mathbf{b}_j$  are the three second-nearest neighbour vectors forming a triangle across a unit cell, and  $M$  is a parameter referring to a modulated potential or a Semenoff mass term [33], which can be implemented e.g. through the presence of a substrate forming a charge density wave. This term is indeed important to induce a different energy shift at the two Dirac points.

This hamiltonian can readily be diagonalized and the

Bloch eigenvectors can be expressed in tensorial product of the eigenstates  $|\pm\rangle = |\pm_{\mathbf{d}_k}\rangle$  of the operator  $\mathbf{d}_k \cdot \boldsymbol{\sigma}$  with eigenvalues  $\pm|\mathbf{d}_k|$ , tensored with the eigenvectors  $|\downarrow_x\rangle$  of the operator  $s_x$  with eigenvalues  $\pm 1$ . The resulting four possibly overlapping bands are

$$E_{\downarrow_x, -}(\mathbf{k}) = -|\mathbf{d}_k| - r \quad (7)$$

$$E_{\downarrow_x, +}(\mathbf{k}) = +|\mathbf{d}_k| - r \quad (8)$$

$$E_{\uparrow_x, -}(\mathbf{k}) = -|\mathbf{d}_k| + r \quad (9)$$

$$E_{\uparrow_x, +}(\mathbf{k}) = +|\mathbf{d}_k| + r. \quad (10)$$

The semimetallic regime is reached when the two middle bands overlap forming a closed one-dimensional Fermi surface denoted as nodal ring. An important prerequisite to observe the formation of a nodal metallic Fermi liquid is that when solving the equation  $\mathcal{H}^2(\mathbf{k}) = 0 = (-r + |\mathbf{d}|)^2$  this leads to two degenerate solutions corresponding to the two eigenstates  $|\uparrow_x\rangle \otimes |-\rangle$  and  $|\downarrow_x\rangle \otimes |+\rangle$  such that  $2r\mathbf{d} \cdot \boldsymbol{\sigma} \otimes s_x = -2r|\mathbf{d}|$ . The semimetal occurs for the range of parameters  $3\sqrt{3}t_2 - M < r < 3\sqrt{3}t_2 + M$  [18]. We remind that  $3\sqrt{3}t_2$  in the Haldane model refers to  $|d_z|$  at the two Dirac points while  $d_x, d_y = 0$ .

### III. QUANTUM HALL RESPONSE AND INVARIANTS

In the linear response regime, the Kubo formula for the Hall conductivity of a 2D electron gas reads [1]

$$\begin{aligned} \sigma^{xy} &= ie^2\hbar \iint_{BZ} \frac{d^2\mathbf{k}}{(2\pi)^2} \sum_{n \neq m} \frac{f(E_n(\mathbf{k}))}{(E_n(\mathbf{k}) - E_m(\mathbf{k}))^2} \quad (11) \\ &\times (\langle n\mathbf{k}|v^x|m\mathbf{k}\rangle \langle m\mathbf{k}|v^y|n\mathbf{k}\rangle - \langle n\mathbf{k}|v^y|m\mathbf{k}\rangle \langle m\mathbf{k}|v^x|n\mathbf{k}\rangle) \end{aligned}$$

where the indices  $n = \downarrow_x, \pm$  and  $m = \uparrow_x, \pm'$  run over the four bands of the system, and  $f(x) = \theta(x)$  is the Fermi-Dirac distribution function being equal to the Heaviside step function at zero temperature.

One may question the applicability of this formula in the semimetallic regime for which bands  $\downarrow_x, +$  and  $\uparrow_x, -$  cross zero energy such that  $E_n(\mathbf{k}) - E_m(\mathbf{k}) = 0$ . Here, a divergence does not occur because the current operator

$$v^\alpha = \frac{1}{\hbar} \partial_{k_\alpha} \mathcal{H} \otimes \mathbb{I}, \quad (12)$$

shows the important property  $\langle \uparrow_x, - | v^\alpha | \downarrow_x, + \rangle = 0$ . Eq. (12) is thus well defined and we can rewrite this expression in terms of the integral of the Berry curvature on the Brillouin zone and all occupied states

$$\sigma^{xy} = \frac{e^2}{\hbar} \iint_{BZ} \frac{d^2\mathbf{k}}{2\pi} \sum_n f(E_n(\mathbf{k})) \mathcal{B}_{n\mathbf{k}} \quad (13)$$

where the Berry curvature of band  $n$  is defined as [34]

$$\mathcal{B}_{n\mathbf{k}} = i(\partial_{k_x} \langle n| \partial_{k_y} |n\rangle - \partial_{k_y} \langle n| \partial_{k_x} |n\rangle). \quad (14)$$

In the semimetallic regime, the contribution from the Fermi-Dirac distribution with the term  $f(E_n(\mathbf{k}))$  appearing in Eq. (13) plays a major role as it constrains the integration to be performed only partially over the Brillouin zone for the two middle bands  $n = \downarrow_x, +$  and  $n = \uparrow_x, -$  which correspond to two partially filled bands, while the integration is performed over the entire Brillouin zone for  $n = \downarrow_x, -$  whose band is entirely filled. This expression gives

$$\sigma^{xy} = \frac{e^2}{\hbar} \left( C_{\downarrow_x, -} + \hat{C}_{\uparrow_x, -} + \tilde{C}_{\downarrow_x, +} \right) \quad (15)$$

for which we have defined (hat and tilde symbols)

$$C_n = \frac{1}{2\pi} \iint_{BZ} d^2\mathbf{k} \mathcal{B}_{n\mathbf{k}} \quad (16)$$

$$\hat{C}_n = \frac{1}{2\pi} \iint_{\overline{NR}} d^2\mathbf{k} \mathcal{B}_{n\mathbf{k}} \quad (17)$$

$$\tilde{C}_n = \frac{1}{2\pi} \iint_{NR} d^2\mathbf{k} \mathcal{B}_{n\mathbf{k}}. \quad (18)$$

In these three expressions, only the regions of integration differ. For the regular Chern number  $C_n$ , the integral is performed over  $BZ$  the entire Brillouin zone, while it is done over the region  $\overline{NR}$  outside the nodal ring for  $\hat{C}_n$  and over the region  $NR$  inside the nodal ring for  $\tilde{C}_n$ . The first integral running on the whole Brillouin zone refers to the lowest energy band which is characterized through an integer topological number similarly as in the Haldane model, assuming that  $3\sqrt{3}t_2 > M$ .

From a mathematical point of view, it is useful to formulate a correspondence from the Brillouin zone to 2-sphere. The same map will also clarify the response to circularly polarized light in the next Section. The  $\mathbf{d}_k$  vector appearing in the Hamiltonian of Eq. (3) gives us the following well defined mapping from the Brillouin Zone to 2-sphere

$$\begin{aligned} \Phi : BZ &\rightarrow S^2 \\ \mathbf{k} &\mapsto (\theta_{\mathbf{k}}, \varphi_{\mathbf{k}}) \end{aligned} \quad (19)$$

where  $(\theta_{\mathbf{k}}, \varphi_{\mathbf{k}})$  are the two uniquely defined angles on  $S^2 = [0, \pi[ \times [0, 2\pi[$  such that

$$\mathbf{d}_k = |\mathbf{d}_k| \begin{pmatrix} \sin \theta_{\mathbf{k}} \cos \varphi_{\mathbf{k}} \\ \sin \theta_{\mathbf{k}} \sin \varphi_{\mathbf{k}} \\ \cos \theta_{\mathbf{k}} \end{pmatrix}. \quad (20)$$

Here,  $\varphi_{\mathbf{k}}$  and  $\theta_{\mathbf{k}}$  are thus the azimuthal and polar angles of the three-dimensional vector  $\mathbf{d}_k$ . This map gives us also the following exact expressions (with no approximations)

$$\mathcal{B}_{\downarrow_x, -, \mathbf{k}} = -\frac{1}{2} \sin \theta_{\mathbf{k}} (\partial_{k_x} \theta_{\mathbf{k}} \partial_{k_y} \varphi_{\mathbf{k}} - \partial_{k_x} \varphi_{\mathbf{k}} \partial_{k_y} \theta_{\mathbf{k}}) \quad (21)$$

$$\mathcal{B}_{\uparrow_x, +, \mathbf{k}} = +\frac{1}{2} \sin \theta_{\mathbf{k}} (\partial_{k_x} \theta_{\mathbf{k}} \partial_{k_y} \varphi_{\mathbf{k}} - \partial_{k_x} \varphi_{\mathbf{k}} \partial_{k_y} \theta_{\mathbf{k}}) \quad (22)$$

$$\mathcal{B}_{\downarrow_x, \pm, \mathbf{k}} = \mathcal{B}_{\uparrow_x, \pm, \mathbf{k}}. \quad (23)$$

We can then integrate by change of variables  $\mathbf{k} \rightarrow (\theta, \varphi)$ . The Fermi surface formed by the nodal ring can be expressed to a good approximation in these variables by the contour  $\theta = \theta_c, \varphi \in [0, 2\pi]$  for a given  $\theta_c$  fixed between 0 and  $\pi$  depending on the value of  $r$ , which defines the position of the nodal ring in the Brillouin zone.

We get by change of variables

$$\begin{aligned}\tilde{C}_{\downarrow x,+} &= \left( \frac{1}{2\pi} \int_0^{2\pi} d\varphi \right) \int_{\theta_c}^{\pi} d\theta \left( +\frac{1}{2} \right) \sin \theta \\ &= \frac{1}{2} [\cos \theta_c + 1]\end{aligned}\quad (24)$$

$$\begin{aligned}\hat{C}_{\uparrow x,-} &= \left( \frac{1}{2\pi} \int_0^{2\pi} d\varphi \right) \int_0^{\theta_c} d\theta \left( -\frac{1}{2} \right) \sin \theta \\ &= \frac{1}{2} (\cos \theta_c - 1)\end{aligned}\quad (25)$$

$$\begin{aligned}C_{\downarrow x,-} &= \left( \frac{1}{2\pi} \int_0^{2\pi} d\varphi \right) \int_0^{\pi} d\theta \left( -\frac{1}{2} \right) \sin \theta \\ &= -1,\end{aligned}\quad (26)$$

which gives us the resulting hall conductivity

$$\begin{aligned}\sigma^{xy} &= \sigma_{\downarrow x,-}^{xy} + \hat{\sigma}_{\uparrow x,-}^{xy} + \tilde{\sigma}_{\downarrow x,+}^{xy} \\ &= \frac{e^2}{h} (\cos \theta_c - 1).\end{aligned}\quad (27)$$

This expression interpolates between  $\sigma^{xy} = -2\frac{e^2}{h}$  for the topological insulating phase when  $r < 3\sqrt{3}t_2 - M$  for which  $\theta_c = \pi$  all the way to  $\sigma^{xy} = 0$  for the trivial insulating phase when  $r > 3\sqrt{3}t_2 + M$  for which  $\theta_c = 0$ . The nodal ring equivalently navigates from the vicinity of  $K'$  towards  $K$  when increasing  $r$  within the semimetal region such that  $3\sqrt{3}t_2 - M < r < 3\sqrt{3}t_2 + M$ . However, the quantized invariant for the  $C_{\downarrow x,-}$  term associated to the lowest-energy band characterizes the presence and robustness of the zero-energy edge mode and can therefore represent a good marker for this topological system. Now, regarding the other two terms traducing the Berry flux accumulated by particles moving around the Fermi surface [21], we can in fact also introduce a quantized  $\mathbb{Z}_2$  invariant, valid for all range of parameters within the semimetal metal phase, such that

$$\hat{C}_{\uparrow x,-} - \tilde{C}_{\downarrow x,+} = C_{\downarrow x,-}. \quad (28)$$

In this sense, we can introduce two invariants to characterize this energy band structure i.e. the  $\mathbb{Z}$  quantized invariant related to the lowest energy band and a  $\mathbb{Z}_2$  index formed through the second-energy band and the nodal ring region or Fermi surface.

Below, we show that the quantized topological response of the lowest band associated to  $C_{\downarrow x,-}$  can be measured through circularly polarized light which then reveals the presence of the robust edge mode. We will also show that this response locally measured from the

resonance at the Dirac points is mathematically equivalent to fix  $\theta_c = \frac{\pi}{2}$  on a sphere i.e. revealing a half-Skyrmion, linking with the physics of the bilayer model [22, 23].

#### IV. TOPOLOGICAL INVARIANTS FROM CIRCULARLY POLARIZED LIGHT

Here, we measure the topological response from a circularly polarized light field in the plane [3, 5, 6, 31] localized resolved in frequency to reach the Dirac point(s). We begin with one plane described through a Haldane model within the topological phase to fix the definitions. Within the Dirac approximation, we take the same definitions of the Brillouin zone as in [5, 31], such that the (photo-induced) current operator takes the form,

$$\hat{J}_{\zeta}(t) = v_F(p_x + A_x(t))\sigma_y - (\zeta p_y + A_y(t))\sigma_x \quad (29)$$

with the velocity  $v_F = \frac{3}{2\hbar}ta$  and  $\mathbf{p} = (p_x, p_y)$  measures a small deviation from the Dirac points. Here,  $\zeta = \pm 1$  at the  $K$  and  $K'$  respectively such that within the choice of the Brillouin zone the two Dirac points are related through  $p_y \rightarrow -p_y$  or more generally  $k_y \rightarrow -k_y$ . The vector potential due to the classical light source is included through a shift of the momentum. There is a subtlety to mention here:  $\zeta$  refers both to the direction of light polarization, right-handed (+) or left-handed (-), and to the Dirac points of interest such that

$$\begin{aligned}\text{Re}A_x &= A_0 \cos(\omega t) \\ \text{Re}A_y &= -\zeta A_0 \sin(\omega t).\end{aligned}\quad (30)$$

The light-matter Hamiltonian can be written in analogy to a spin-1/2 particle where  $\sigma^+$  and  $\sigma^-$  operators correspond to light-induced hopping terms from one to the other sublattice in the plane [5, 6, 31]. Within the topological phase of the Haldane model, due to the energy conservation and inversion effects between the specific form of eigenstates at the two Dirac points [6, 31], the right-handed circular polarization interacts with one Dirac point and the left-handed circular polarization interacts with the other Dirac point. From the form of the Dirac Hamiltonian for one layer we also have

$$\begin{aligned}\sigma_x &= \frac{1}{\hbar v_F} \frac{\partial \mathcal{H}}{\partial p_x} \\ \sigma_y &= \frac{1}{\hbar v_F} \frac{\partial \mathcal{H}}{\partial (\zeta p_y)}.\end{aligned}\quad (31)$$

$$\hat{J}_{\zeta}(t) = (p_x + A_x(t)) \frac{\partial \mathcal{H}}{\hbar \partial (\zeta p_y)} - (\zeta p_y + A_y(t)) \frac{\partial \mathcal{H}}{\hbar \partial p_x}. \quad (32)$$

Since we will evaluate the linear response to second-order in  $A_0$ , as if we just keep the terms in  $A_x(t)$  and  $A_y(t)$  in this formula, this is equivalent to measure the light-induced response at the Dirac points with here

$p_x = p_y = 0$  and to average on all the wavevectors within the Brillouin zone [3]. Therefore, this results in the form of the current operator

$$\hat{J}_\zeta(t) = \frac{1}{2\hbar} A_0 e^{-i\omega t} \left( \frac{\partial \mathcal{H}}{\partial(\zeta p_y)} + \zeta i \frac{\partial \mathcal{H}}{\partial p_x} \right) + h.c. \quad (33)$$

For the Haldane model, this leads to the following response associated to the *photo-induced currents* [5, 31]

$$\Gamma_\zeta(\omega) = \frac{2\pi A_0^2}{\hbar} \frac{1}{2} \left| \langle + | \left( \frac{\partial \mathcal{H}}{\partial(\zeta p_y)} + \zeta i \frac{\partial \mathcal{H}}{\partial p_x} \right) | - \rangle \right|^2 \times \delta(E_l(\mathbf{p}) - E_u(\mathbf{p}) - \hbar\omega). \quad (34)$$

The symbol  $\zeta$  only occurs through  $\zeta^2 = 1$  which means that it can be dropped at this step of the calculation. It is then important to remind here that we have the correspondences of eigenstates  $|+\rangle_K \leftrightarrow |-\rangle_{K'}$  and  $|-\rangle_K \leftrightarrow |+\rangle_{K'}$  for the Haldane model such that the crossed terms result in a finite number when measuring  $\Gamma_+(\omega) - \Gamma_-(\omega)$ . The energy conservation is taken into account through the definition of  $A_y$  such that at this step the  $\delta$ -function is applicable close to both Dirac points;  $E_l$  and  $E_u$  refer to the lower and upper energy bands with energy  $\pm|\mathbf{d}|$  in the Haldane model. These crossed terms are precisely related to the function entering into the quantum Hall response since we can introduce precisely the velocities  $v^x$  and  $v^y$  of the preceding Section. We show below that it is possible to find a resonance condition for one light polarization only setting  $E_u(K) - E_l(K) = \hbar\omega$  with  $\mathbf{p} \rightarrow \mathbf{0}$ . This implicitly assumes to have a precise knowledge of the energy spectrum from other measures. In this way, we can equivalently (mathematically) integrate on all frequencies since the  $\delta$ -function is zero when  $E_u - E_l \neq \hbar\omega$ . Then, this results in a quantized circular dichroism response related to the topological invariant of the lowest and upper bands  $C = \mp 1$  [3, 5, 6, 31]

$$\left| \frac{\Gamma_+ - \Gamma_-}{2} \right| = \frac{2\pi}{\hbar} A_0^2 |C|, \quad (35)$$

which can be then equivalently resolved from the information at the Dirac points. It is also relevant to mention that finding the resonance with the  $M$  point(s) or (equivalently  $\Gamma$ -point) this would result in a half-quantized response [6].

Below, we show that the response to circularly polarized light remains meaningful for the topological semimetal, from the  $K$  and  $K'$  points Dirac theory. For the topological semimetal, within the Dirac approximation for the  $d_x(\mathbf{k})$  and  $d_y(\mathbf{k})$  terms, the Hamiltonian takes the form

$$\mathcal{H}(\mathbf{p}) = (\hbar v_F (p_x \sigma_x + \zeta p_y \sigma_y) + (\zeta d_z + M) \sigma_z) \otimes \mathbb{I} + r \mathbb{I} \otimes s_x. \quad (36)$$

We introduce precisely identity matrices  $\mathbb{I}$  which act in the sublattice and spin Hilbert spaces. Therefore, we can yet write down  $\sigma_x \otimes \mathbb{I} = \frac{1}{\hbar v_F} \frac{\partial \mathcal{H}}{\partial p_x} \otimes \mathbb{I}$  and  $\sigma_y \otimes \mathbb{I} =$

$\frac{1}{\hbar v_F} \frac{\partial \mathcal{H}}{\partial(\zeta p_y)} \otimes \mathbb{I}$ . The current operator then takes the form

$$\hat{J}_\zeta(t) = \left( \frac{1}{2\hbar} A_0 e^{-i\omega t} \left( \frac{\partial \mathcal{H}}{\partial(\zeta p_y)} + \zeta i \frac{\partial \mathcal{H}}{\partial p_x} \right) + h.c. \right) \otimes \mathbb{I}. \quad (37)$$

Since we have an identity matrix in the spin sector, within our definitions, this refers to the current of a spin- $\uparrow_z$  or spin- $\downarrow_z$  particle equally. We verify below through justifications from the band structure that since we have an identity operator in the spin space for the current it gives equal currents for a spin- $\uparrow_x$  or spin- $\downarrow_x$  particle.

An important point is to incorporate the energy conservation within the four-energy bands model. It is then useful to write down the light-matter interaction  $\delta H_\pm = A_0 e^{\pm i\omega t} \sigma^\pm \otimes \mathbb{I}$  within the four energy bands. Since the light-matter interaction couples bands with the same spin quantum number this implies that at the  $K$ -point this will only mediate transitions between bands  $n = \downarrow_x, -$  and band  $m = \downarrow_x, +$  and separately between bands  $n' = \uparrow_x, -$  and band  $m' = \uparrow_x, +$ . Interestingly, it is possible to find a resonance with both pairs of bands fixing the light frequency such that  $\hbar\omega = 2|d_z(K)| = 6\sqrt{3}t_2 + 2M$  for the right-handed wave (+). It is interesting to observe that in the present case, it is possible to fix the resonant condition just with the  $K$  Dirac point.

Due to the structure of eigenstates in the valley around the  $K$  Dirac point, only one of the two light polarizations, e.g. the right-handed polarization, will be able to mediate inter-band transitions similarly to the topological two-bands model. Thus, due to the identification between eigenstates  $|\uparrow_z\rangle = \frac{1}{\sqrt{2}}(|\uparrow_x\rangle + |\downarrow_x\rangle)$  and  $|\downarrow_z\rangle = \frac{1}{\sqrt{2}}(|\uparrow_x\rangle - |\downarrow_x\rangle)$ , we deduce that the inter-band transitions for one spin polarization  $\uparrow_z$  or  $\downarrow_z$  will then correspond effectively to a half of the sum of the transition rates associated to the two pairs of bands  $(n, m)$  and  $(n', m')$  respectively, which are in fact equal. Therefore, for the topological semimetal, the response at the  $K$  point for the + light polarization is identical to Eq. (34) for each spin polarization  $|\uparrow_z\rangle$ ,  $|\downarrow_z\rangle$  or for each pair of bands  $(n, m)$  and  $(n', m')$  corresponding to spin polarizations  $|\downarrow_x\rangle$  and  $|\uparrow_x\rangle$  respectively.

At the  $K'$  point, the two occupied bands ( $n$  and  $m$ ) at zero temperature have the same spin polarization whereas the two empty bands ( $n'$  and  $m'$ ) have now a distinct spin polarization, as shown in Fig. 1. Therefore, to mediate inter-band transitions towards empty states in the quantum limit, this would require to also flip the spin polarization of an electron. Therefore, in the presence of the light field, due to the two-particles ground-state structure at the  $K'$  point, this results in  $\Gamma_- = 0$  [31]. Hence, if we define circular dichroism for a pair of energy bands, e.g. related to the first (second) and third (fourth) energy bands at the two Dirac points, we also have  $\Gamma_- = 0$  for these pairs at finite temperature. It is then useful to analyze the information in  $\Gamma_+$  at the  $K$  point in Eq. (34) through the Berry curvature  $F_{p_x p_y}$  mapped onto the 2-sphere [31]. The  $K$  Dirac point corresponds to north pole and  $K'$  to south pole along

the polar angle direction. There is then a simple relation between the Berry curvature in the plane and the pseudo-spin variable [6]

$$F_{p_x p_y} = \frac{2(\hbar v_F)^2}{|E_u - E_l|^2} \cos \theta = \frac{2(\hbar v_F)^2}{|E_u - E_l|^2} \langle \sigma_z(\theta) \rangle \quad (38)$$

where for the topological semimetal, at the  $K$  point,  $E_u - E_l = E_m - E_n = E_{m'} - E_{n'}$ . Therefore, at the  $K$  point for a spin polarization  $\uparrow_z, \downarrow_z$  or a pair of bands  $(n, m)$  and  $(n', m')$  we have

$$\left| \frac{\Gamma_+}{2} \right| = \frac{2\pi}{\hbar} A_0^2 \frac{1}{2} \langle \sigma_z(0) \rangle. \quad (39)$$

Since at the  $K'$  point,  $\Gamma_- = 0$  then this is equivalent to

$$\left| \frac{\Gamma_+ - \Gamma_-}{2} \right| = \frac{2\pi}{\hbar} A_0^2 \frac{1}{2} |\langle \sigma_z(0) \rangle|. \quad (40)$$

Here,  $\sigma_z$  measures the relative density on the two sublattices of the honeycomb lattice resolved at the  $K$  Dirac point. In comparison, for the Haldane model, we obtain

$$\begin{aligned} \left| \frac{\Gamma_+ - \Gamma_-}{2} \right| &= \frac{2\pi}{\hbar} A_0^2 \frac{1}{2} |(\langle \sigma_z(0) \rangle - \langle \sigma_z(\pi) \rangle)| \\ &= \frac{2\pi}{\hbar} A_0^2 |\langle \sigma_z(0) \rangle|. \end{aligned} \quad (41)$$

The topological number of the Haldane model on the 2-sphere takes the equivalent form [31, 35]

$$C = \frac{1}{2} (\langle \sigma_z(0) \rangle - \langle \sigma_z(\pi) \rangle). \quad (42)$$

A peculiarity of this topological semimetal is that  $\langle \sigma_z(\pi) \rangle = 0$  as a result of the formation of the nodal ring semimetal around  $K'$  which is another way to justify why  $\Gamma_- = 0$  in this case. The response for one-spin polarization is now halved compared to one topological plane as a result of  $\Gamma_- = 0$ . The topological semimetal in the bilayer model [22, 23] can be characterized in terms of a pair of one-half local topological markers and  $\pi$ -Berry phases [23] related to the two-spheres' model associated to spin polarizations  $\uparrow_z, \downarrow_z$  [22]. In the one-layer graphene realization, the  $\pi$  Berry phase is associated equally to the phase acquired by an electron with spin polarization  $\uparrow_x$  in band 2 and by an electron with spin polarization  $\downarrow_x$  in band 1, when circling around the  $K$  Dirac. A pair of  $\pi$ -Berry phases is also analogous to a pair of  $\pi$  winding numbers. A  $\frac{1}{2}$  light response is also predicted to occur for the  $\nu = \frac{1}{2}$ -fractional quantum Hall effect [36].

If we sum the information on these two spin polarizations (or equally  $\uparrow_z, \downarrow_z$ ) i.e. on the two pairs of bands  $(n, m)$  and  $(n', m')$ , we now have

$$\sum_{j=\uparrow, \downarrow} \left| \frac{\Gamma_+ - \Gamma_-}{2} \right| = \frac{2\pi}{\hbar} A_0^2 \cos(\theta = 0). \quad (43)$$

Now, we can establish a precise relation with the quantum Hall response of the lowest energy band in Eq. (27) through

$$C_{\downarrow_x, -} = \frac{1}{2} (\cos(\pi) - \cos(0)) = -\cos(0) = -1. \quad (44)$$

Therefore, we obtain a relation between light and topological response associated to the lowest-energy band

$$\sum_{j=\uparrow, \downarrow} \left| \frac{\Gamma_+ - \Gamma_-}{2} \right| = \frac{2\pi}{\hbar} A_0^2 |C_{\downarrow_x, -}|. \quad (45)$$

When  $r < 3\sqrt{3}t_2 - M$ , the same light polarization would equally interact with both pairs  $(n, m)$  and  $(n', m')$  at one Dirac point measuring twice the topological invariant of the lowest band, in agreement with the quantum Hall conductivity. For  $r > 3\sqrt{3}t_2 - M$ , one pair of bands will interact with one distinct light polarization at each Dirac point. In this case, if we reproduce the steps of the calculation above we now find that  $\Gamma_+ - \Gamma_- = 0$  at each Dirac point. In Eq. (32), the two pairs  $(n, m)$  and  $(n', m')$  are now characterized with different signs of  $A_y(t)$  and inverted lower and upper energy eigenstates, for the same Dirac point.

We have reminded above that the light response at the  $K$  and  $K'$  points for the topological Haldane model reveals the same information as the light response and therefore the quantum Hall response coming from a summation on the whole Brillouin zone [31]. This identification necessitates that the quantum Hall responses and light responses are continuous and differentiable everywhere. For the topological semimetal, this requires that the intermediate bands do not alter the result from the lowest-energy band in Sec. III. In this way, the light response from the Dirac points is identical to the quantum Hall response of the semimetal only if  $\theta_c = \frac{\pi}{2}$ . For  $\theta_c = \frac{\pi}{2}$ , we also observe that the quantum Hall response coming from  $\uparrow_x$  particles in the second-energy band takes the form  $\frac{e^2}{h} \hat{C}_{\uparrow_x, -} = -\frac{1}{2} \frac{e^2}{h}$  [23]. Similarly, if we now sum the topological number associated to the  $\downarrow_x$  particles in the two energy bands, this also measures  $\frac{e^2}{h} (\hat{C}_{\downarrow_x, +} + \hat{C}_{\downarrow_x, -}) = -\frac{1}{2} \frac{e^2}{h}$  and gives a similar interpretation to the other half-topological number. The light approach then equivalently measures the topological response  $\sum_{j=\uparrow, \downarrow} C_\alpha$  with  $|C_\alpha| = \frac{1}{2}$ , in relation with the bilayer model [18, 22, 23].

## V. BULK-EDGE CORRESPONDANCE

The topological semimetal of interest in this paper can also be understood as a superposition of two Haldane models associated here to each spin polarization towards the axis of the in-plane magnetic field corresponding to the axis of the in-plane magnetic field corresponding to the  $r\mathbb{I} \otimes s_x$  term in the Hamiltonian of Eq. (3). This magnetic field of small amplitude polarizes the system into two subsystems which are independent of each other as long as the  $\mathbb{Z}_2$  symmetry of the Hamiltonian is preserved.

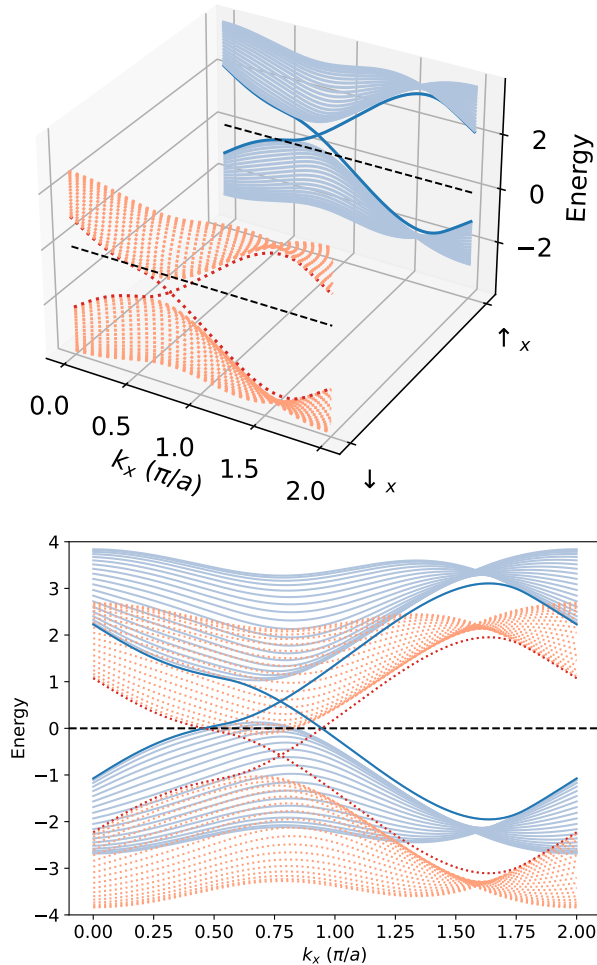


Figure 2. Color online: (Above) One-dimensional energy bands of the topological semimetal showing the two underlying band structures of opposite spin polarization, with the spin polarization shown in the third direction. (Bottom) Resulting energy bands in the momentum-Energy axis. The parameters chosen for all panels are  $M = 3\sqrt{3}t/4$ ,  $r = t/\sqrt{3}$ ,  $t_2 = t/3$  with  $a = 1$ .

As shown in the upper panel of Fig. 2, these two subcopies of the Haldane model are of the same topological nature in the sense that the lower bands have the same Berry curvature and hence the same Chern number, but the bands of the two subsystems are not filled evenly. The second band of the  $\downarrow_x$  population is partially filled while the first band of the  $\uparrow_x$  population is partially filled symmetrically to the  $\downarrow_x$  population. As long as the  $\mathbb{Z}_2$  symmetry of the system is preserved, the two subsystems are well defined and the lower band of the  $\uparrow_x$  population does not mix to the upper band of the  $\downarrow_x$  population, and no gap is opened in the band structure.

The topological nature of this semimetal comes from the fact that each of the spin subsystem acts as if its chemical potential was shifted by  $\pm r$  from its half-filling value, which leads for the bands to be either emptied or

filled in a symmetric way between the two subsystems. This does not change however the topological nature of the bands themselves which keep their Berry curvature and their resulting Chern number. The topological nature of the bands is well defined here in terms of Chern number, but the resulting band structure is gapless when taking the two spin populations together. Spin resolved Angle Resolved PhotoEmission Spectroscopy (ARPES) appears as the most simple and decisive way to probe this semimetal. This should allow us to retrieve the band structure of each spin population independently, and thus to characterize the topological nature of each spin population on its own. This approach should also allow for example to reproduce the topological nature of the spin Hall phase for the case of the Kane-Mele model.

Another way to probe this semimetal is using spin-polarized transport at chemical potential  $\mu$  which satisfies  $|\mu \pm r| < |M - 3\sqrt{3}t_2|$ . Indeed, the spin polarization of the system in the  $x$  direction is a well defined quantum number and in such a regime for the chemical potential, the mesoscopic Hall conductance of one spin population is quantized due to the unique presence of spin-polarized edge modes while the conductance of the other population is non quantized due to the presence of spin-polarized bulk modes at this regime of chemical potential. If we consider the graphic representations of the energy bands in Fig. 2, the system can thus be seen in this regime of chemical potential as a half-topological semimetal: one spin population is in the topological insulating phase while the other is in a metallic regime. One quantized edge mode also agrees with the quantum Hall response of the lowest energy band. We also emphasize here that the presence of a quantized conductance at the edges for one spin-population polarized along  $x$  direction is also equivalent to a  $\frac{1}{2} - \frac{1}{2}$  conductance for the two spin polarizations along  $z$  direction which is precisely at the heart of the bulk-edge correspondence interpretation for the bilayer model [22, 23] and the  $\mathbb{Z}_2$  symmetry associated to the two spin polarizations along  $z$  direction.

## VI. CONCLUSION

To summarize, the quantum Hall conductivity of the recently identified two-dimensional topological nodal ring semimetal on the honeycomb lattice in one-layer graphene reveals a  $\mathbb{Z}$  topological invariant  $C_{\downarrow_x,-}$  associated to the lowest-energy band and a  $\mathbb{Z}_2$  spin Chern number  $\hat{C}_{\uparrow_x,-} - \hat{C}_{\downarrow_x,+}$  for the partially filled bands. The specificity of the topological semimetal phase resides in the occurrence of a gap closing region at the Fermi energy due to crossing between two bands which in the present case is also characterized through a  $\mathbb{Z}_2$  spin Chern number in addition to the quantized quantum Hall response. We evaluated the response to circularly polarized light, which is an equivalent marker of the topological response and of the quantum Hall conductivity for the Haldane model, and showed how this can yet reveal the quan-

tum Hall conductivity for the lowest-energy band of the topological semimetal from the frequency resonance corresponding to the energy gap at the Dirac points.

We have then justified that this system is a half-topological semimetal, i.e. one spin population along  $x$  direction being in the topological insulating phase while the other is in a metallic regime resulting in a conductance at the edges quantized for one spin-polarization only. The quantized edge mode then has a  $1/2$  probability to be in the  $\uparrow_z, \downarrow_z$  state associated to the original basis of the Hamiltonian. These results can be verified through spin-polarized transport at the edges and spin-polarized ARPES. The approach for the light-matter interaction resolved in the two Dirac valleys is also equivalent to a pair of one-half topological numbers associated to  $\uparrow_z$  or  $\downarrow_z$  spin polarizations, linking with the physical properties of the topological semimetal on the bilayer model [22, 23].

We also mention here that one-half topological numbers also find applications for the physics of interacting topological superconducting p-wave wires [37] and the physics of Majorana fermions [23, 38].

These protected topological semimetals present then two different flows of charges, associated to a two-dimensional Fermi liquid in the bulk and a one-dimensional (protected) channel(s) at the edges which may find applications in electronics and energy.

We acknowledge useful discussions with Joel Hutchinson, Andrej Mesaros and Michel Ferrero for interesting discussions. This work was supported by the french ANR BOCA and the Deutsche Forschungsgemeinschaft (DFG), German Research Foundation under Project No. 277974659. Sariah Al Saati thanks Ecole Polytechnique for funding his PhD thesis.

- 
- [1] D. J. Thouless, M. Kohmoto, M. P. Nightingale, and M. den Nijs, *Physical Review Letters* **49**, 405 (1982).
- [2] M. Kohmoto, *Annals of Physics* **160**, 343 (1985).
- [3] D. T. Tran, A. Dauphin, A. G. Grushin, P. Zoller, and N. Goldman, *Science Advances* **3** (2017).
- [4] L. Asteria, D. T. Tran, T. Ozawa, M. Tarnowski, B. S. Rem, N. Flaschner, K. Sengstock, N. Goldman, and C. Weitenberg, *Nature Physics* **15**, 449 (2019).
- [5] P. W. Klein, A. Grushin, and K. Le Hur, *Phys. Rev. B* **103**, 035114 (2021).
- [6] K. Le Hur, *Phys. Rev. B* **105**, 125106 (2022).
- [7] J. Legendre and K. Le Hur, *Phys. Rev. A Letter* **109**, L021701 (2024).
- [8] M. Dyakonov and V. Perel, *Soviet Journal of Experimental and Theoretical Physics Letters* **13**, 467 (1971).
- [9] S. Murakami, N. Nagaosa, and S.-C. Zhang, *Science* **301**, 1348 (2003).
- [10] C. L. Kane and E. J. Mele, *Physical Review Letters* **95**, 226801 (2005).
- [11] C. L. Kane and E. J. Mele, *Physical Review Letters* **95**, 146802 (2005).
- [12] S. Rachel and K. Le Hur, *Phys. Rev. B* **82**, 075106 (2010).
- [13] W. Wu, S. Rachel, W.-M. Liu, and K. Le Hur, *Phys. Rev. B* **85**, 205102 (2012).
- [14] M. Hohenadler, T. C. Lang, and F. F. Assaad, *Phys. Rev. B* **106**, 100403 (2011).
- [15] B. A. Bernevig and S.-C. Zhang, *Physical Review Letters* **96**, 106802 (2006).
- [16] L. Sheng, D. N. Sheng, C. S. Ting, and F. D. M. Haldane, *Phys. Rev. Lett.* **95**, 136602 (2005).
- [17] L. Fu and C. L. Kane, *Phys. Rev. B* **76**, 045302 (2007).
- [18] K. Le Hur and S. Al Saati, *Physical Review B* **107**, 165407 (2023).
- [19] J. Hutchinson, P. W. Klein, and K. Le Hur, *Phys. Rev. B* **104**, 075120 (2021).
- [20] I. Titvinidze, J. Legendre, K. Le Hur, and W. Hofstetter, *Phys. Rev. B* **105**, 235102 (2022).
- [21] F. D. M. Haldane, *Physical Review Letters* **93**, 206602 (2004).
- [22] J. Hutchinson and K. Le Hur, *Communications Physics* **4**, 144 (2021).
- [23] K. Le Hur, *Phys. Rev. B* **108**, 235144 (2023).
- [24] F. D. M. Haldane, *Physical Review Letters* **61**, 2015 (1988).
- [25] P. Cheng, P. W. Klein, K. Plekhanov, K. Sengstock, M. Aidelsburger, C. Weitenberg, and K. Le Hur, *Phys. Rev. B(R)* **100**, 081107(R) (2019).
- [26] J.-H. Zheng and W. Hofstetter, *Phys. Rev. B* **195434**, 195434 (2018).
- [27] T. H. Hsieh, H. Ishizuka, L. Balents, and T. Hughes, *Phys. Rev. Lett.* **116**, 086802 (2016).
- [28] T. Shoman, A. Takayama, T. Sato, S. Souma, T. Takahashi, T. Oguchi, K. Segawa, and Y. Ando, *Nature Communications* **6**, 6547 (2015).
- [29] Z. Wang, D. Ki, H. Chen, H. Berger, A. H. MacDonald, and A. F. Morpurgo, *Nature Communications* **6**, Article number:8339 (2015).
- [30] P. Tiwari, S. K. Srivastav, S. Ray, T. Das, and A. Bid, *ACS Nano* **15**, 916 (2020).
- [31] K. Le Hur, *Review Submitted to Physics Reports, Elsevier, September 2023*, arXiv:2209.15381 (2022).
- [32] J. W. McIver, B. Schulte, F.-U. Stein, T. Matsuyama, G. Jotzu, G. Meier, and A. Cavalleri, *Nature Physics* **16**, 38 (2020).
- [33] G. W. Semenoff, *Physical Review Letters* **53**, 2449 (1984).
- [34] M. V. Berry, *Proceedings of the Royal Society A, Mathematical Physical and Engineering Sciences* **392**, 1802 (1984).
- [35] L. Henriot, A. Sclocchi, P. P. Orth, and K. Le Hur, *Phys. Rev. B* **95**, 054307 (2017).
- [36] C. Repellin and N. Goldman, *Phys. Rev. Lett.* **122**, 166801 (2019).
- [37] F. del Pozo, L. Herviou, and K. Le Hur, *Phys. Rev. B* **107**, 155134 (2023).
- [38] E. Bernhardt, B. Chung Hang Cheung, and K. Le Hur, , arXiv:2309.03127.